Structure and Mechanism in Aerobic Alkene Epoxidations promoted by Ruthenium Complexes of Bis(dihydrooxazole) Ligands†

Simon Bennett,[a] Stephen M. Brown,[b] Gráinne Conole,[c] Margalith Kessler,[c] Simon Rowling,[a] Ekkehard Sinn[a] and Simon Woodward*,[a]

[a] *School of Chemistry, University of Hull, Kingston-upon-Hull HU6 7RX, UK*

[b] *Zeneca FCMO, Leeds Road, Huddersfield HD2 1FF, UK*

[c] *School of Applied Chemistry, University of North London, Holloway Road, London N7 8DB, UK*

Reaction of $[RuCl_2(NCMe)_2(cod)]$ with bis(dihydrooxazoles) gave $[RuCl_2(cod)\{(S,S)\text{-}R^1{}_2C(C{=}NCHR^2CR^1{}_2O)_2\}]$ (cod = cycloocta-1,5-diene; R^1 = H, R^2 = CH_2Ph or Pr^i; R^1 = Me, R^2 = Pr^i). The benzyl complex has been crystallographically characterised. The IR spectra of the complex of the hexamethyl-substituted compound suggest that the ligand is relatively distorted and this is borne out by crystallographic comparison of the model complexes *cis*-$[W(CO)_4\{(S,S)\text{-}R_2C(C{=}NCHPr^iCR_2O)_2\}]$ (R = H or Me). Mechanistic studies of the epoxidation of styrene and stilbenes in the presence of isobutyraldehyde and molecular oxygen using the ruthenium complexes as catalysts in the presence and absence of 4-*tert*-butylcatechol as a radical trap revealed that the metals act as promoters for the production of Pr^iCO_3H and that this carries out the epoxidation, either directly or by formation of oxo-ruthenium species.

A recent flurry of papers describing alkene epoxidation in the presence of molecular oxygen, aliphatic aldehydes (typically isobutyraldehyde, Pr^iCHO), and various metal promoters may be traced to the initial reports of Mukaiyama and co-workers[1–6] using simple metal acetylacetone and Schiff-base-derived catalysts. The high turnover efficiency of these reactions and unusual selectivities compared to traditional methods for dioxygen activation, such as P-450 enzyme mimics,[7] led us to investigate the possibility of exploiting these reactions for asymmetric alkene epoxidations using the bis(dihydrooxazoles)[8] L^1–L^3 and ruthenium centres. Ruthenium complexes have an excellent track record in molecular oxygen activation,[9–13] additionally, the bis(dihydrooxazoles) may be thought of as acetylacetone analogues suggesting a combination of the two should provide efficient epoxidation reactions. This paper describes our initial investigation of the chemistry that drives these efficient epoxidations; this information is complementary to two recent mechanistic studies.[14,15]

Results and Discussion

Ligand Synthesis.—One criterion for obtaining stereoselectivity in metal complex-catalysed oxidation is that the auxiliary chiral ligand must resist oxidative degradation during the reaction. Although there is good precedent for a degree of oxidative resistance at the C(4) stereogenic centres of dihydrooxazoles closely related to L^1 and L^2,[16] this is dramatically improved by substitution at C(5).[17] The simplest oxidatively resistant group one might introduce is to replace CH_2 by CMe_2. Similarly, the activated methylene backbone in these ligands is oxidation sensitive suggesting that superior oxidative stability should arise from its replacement with a CMe_2 unit. Although at the outset of this project no such ligands were known, suitable aminoalcohols may be readily prepared from L-valine (Scheme 1). An example of this class of bis(dihydrooxazole) compound with R = Ph has recently appeared due to Corey and Ishihara.[18] Initially we employed an essentially identical route to the synthesis of the sterically protected L^3. The reactions proceed as expected, excepting that deprotection of the $NHCOCF_3$ amide **III** requires slightly more forcing conditions than normal. Hydrolysis of trifluoroacetamides is often carried out at room temperature, but refluxing in EtOH–water with KOH is required in our case; no racemisation of the chiral centre results. These inelegant protection steps can be avoided by direct formation of diamide **V** followed by treatment with an excess of LiMe to yield **VI**. The former is prepared in quantitative yield from commercially available methyl L-valinate hydrogenchloride **II** and dimethylmalonyl chloride (Scheme 1). Cyclisation of **VI** to the final compound L^3 proceeds in the presence of methanesulfonic acid and molecular sieves to remove water. Occasionally small amounts of a low R_f impure by-product are also obtained the ^1H NMR spectra of which are consistent with only monocyclisation of the bis(amide) **VI**. Compound L^3 has a number of desirable properties: it is crystalline with a melting point significantly above room temperature [many bis(dihydrooxazoles) are oils at ambient temperature]. The ^1H NMR spectrum is rewardingly simple; the isopropyl CH proton is the only multiplet and the only other coupled signal is the RCHN proton appearing as a doublet (J_{HH} = 6.5 Hz). The compound seems more stabilised to hydrolysis compared to normal bis(dihydrooxazoles) (samples of L^3 stored without special precautions are unchanged after at least a year). Most reassuringly the compound shows no sign of degradation or racemisation on prolonged reflux in $CDCl_3$ in the presence of an excess of NiO_2 (the preferred reagent for dihydrooxazole dehydrogenation).[16]

Ruthenium Complexes.—As the original Mukaiyama oxidation reactions had all used simple metal acetylacetone complexes, $M(acac)_n$, as promoters we initially investigated the

† *Supplementary data available* (SUP No. 57057, 5 pp.): Preparation of **I**, **III** and **V**. See Instructions for Authors, *J. Chem. Soc., Dalton Trans.*, 1995, Issue 1, pp. xxv–xxx.

Non-SI unit employed: atm = 101 325 Pa.

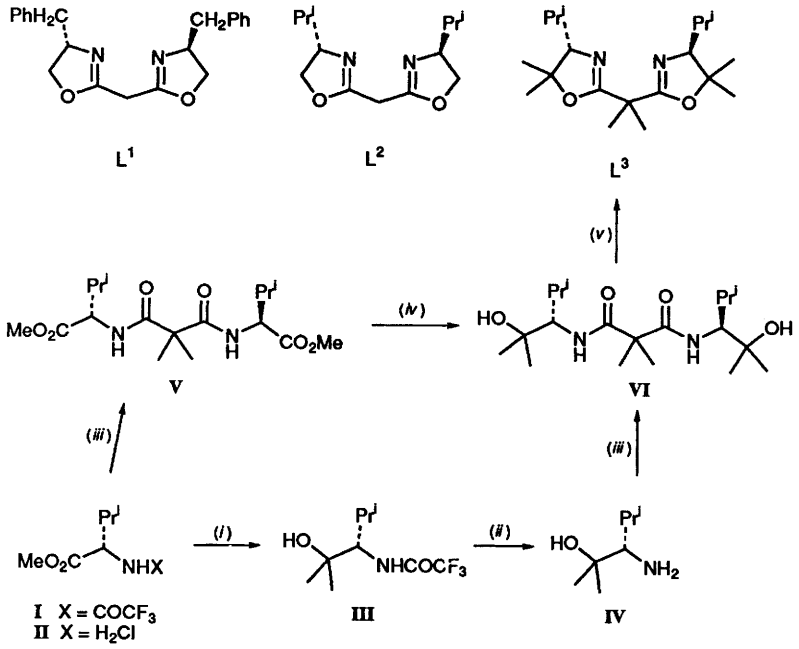

Scheme 1 (*i*) Excess of MgMeI, Et_2O–tetrahydrofuran (thf), 0 °C; (*ii*) KOH–water–EtOH, reflux; (*iii*) dimethylmalonyl chloride–NEt_3, CH_2Cl_2, −78 to 22 °C; (*iv*) excess of LiMe, thf, −78 to 22 °C; (*v*) $MeSO_3H$, A4 molecular sieves, CH_2Cl_2, reflux

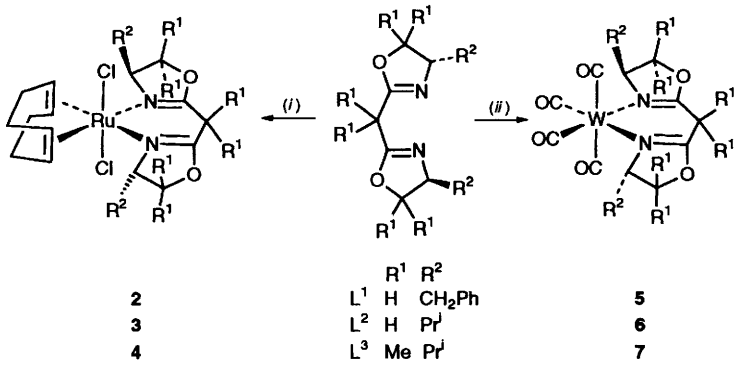

Scheme 2 (*i*) $[RuCl_2(NCMe)_2(cod)]$ **1**, CH_2Cl_2 or MeCN, 22 °C; (*ii*) $[W(CO)_6]$, tetralin (1,2,3,4-tetrahydronaphthalene), 190 °C

reaction of the iron salt $Fe(BF_4)_2$ and the ruthenium complex $[\{RuCl_2(cod)\}_n]$ (cod = cycloocta-1,5-diene) with the anion derived from L^1 *via* methylene deprotonation with LiBu. These preparations give some very substitution-labile air-sensitive intermediates which rapidly oxidise to complex paramagnetic mixtures on exposure to atmospheric oxygen, the actual complexes generated being dependent on the quantity of oxygen present. We have been unable to isolate anything from the iron reactions. Related air-sensitive tetrahedral semicorrin complexes of iron(II) have recently been reported; these are obtained under anaerobic conditions.[19] In reactions with limited amounts of air (O_2 and moisture) contamination during reaction of $[\{RuCl_2(cod)\}_n]$ with the anion of L^1 a deep black-blue solid, apparently $[RuCl_2L^1{}_2]Cl$, is isolated as a toluene solvate. Our assignment of this ruthenium(III) paramagnetic complex is based on its elemental analysis and FAB mass spectrum. The paramagnetically shifted ^1H NMR spectrum of the material is uninformative. Despite many attempts we have been unable to obtain suitable single crystals of this complex to corroborate the hypothesis.

The tendency of protocols based on the anions of L^1 and L^2 to yield intractable paramagnetic mixtures led us to investigate the reactions of *cis-trans*-$[RuCl_2(NCMe)_2(cod)]$ **1**[20] with the neutral compounds, which are expected to give diamagnetic low-spin d^6 ruthenium(II) complexes. These well characterised complexes could be oxidised *in situ* to give competent catalysts for the oxygenation studies. The reaction of **1** with phenylalanine-derived L^1 takes some 7–8 h to proceed to completion at room temperature (Scheme 2). The highest yields of complex **2** are isolated in reactions where 3–4 equivalents of dihydrooxazole are used, the excess being removed from the crude product with MeCN to afford **2** as a free flowing pale yellow powder (Scheme 2). The spectroscopic properties of the isolated material are consistent with a *trans* structure which retains a C_2 rotational axis. In particular, the twelve protons of the co-ordinated cod fall into two equivalent sets of six coupled protons as evidenced by 500 MHz ^1H–^1H correlation spectroscopy (COSY).

These conclusions are reinforced by the results of a crystallographic study of complex **2** which shows the solid-state structure closely related to that in solution. An ORTEP[21] view is shown in Fig. 1, while fractional atomic coordinates, pertinent bond lengths and angles are given in Tables 1 and 2. A *trans* geometry is clearly evident [Cl(1)–Ru–Cl(2) 160.07(6)°] with the chloride ligands bending slightly back towards the methylene group in the bis(dihydrooxazole). Overall the complex is not quite C_2-symmetric in the solid state; crystal-packing effects probably account for the minor deviations. The benzylic fragments orient themselves away from the co-ordinated chlorides to minimise any steric interactions. This conformation may be retained in solution. The chemical shift difference of the two CH_2Ph protons, Δ_{CH_2} 0.7 ppm, is significantly larger than that in free L^1, Δ_{CH_2} 0.43 ppm, suggesting that on average one benzylic proton spends rather

Table 1 Final atomic coordinates for complex **2**

Atom	*x*	*y*	*z*	Occupancy	Atom	*x*	*y*	*z*
Ru	0.183 96(4)	3/4	0.659 01(2)		C(25)	0.085 5(7)	0.976 7(4)	0.671 4(4)
Cl(1)	−0.093 0(1)	0.744 5(2)	0.534 37(7)		C(30)	0.246 9(7)	1.011 3(4)	0.636 2(4)
Cl(2)	0.450 7(2)	0.817 8(1)	0.767 34(9)		C(32)	0.382 4(6)	0.812 1(4)	0.480 6(3)
O(24)	−0.031 7(5)	1.053 3(3)	0.682 5(3)		C(33)	0.498 6(8)	0.906 7(4)	0.468 5(4)
O(34)	0.425 2(5)	0.986 7(3)	0.519 6(2)		C(35)	0.320 5(6)	0.940 8(4)	0.571 9(3)
N(21)	0.047 3(5)	0.886 5(3)	0.696 2(3)		C(50)	0.242 4(9)	0.786 7(5)	0.391 5(5)
N(31)	0.291 7(5)	0.843 5(3)	0.559 0(3)		C(51)	0.321 0(9)	0.778 6(4)	0.302 6(4)
C(1d)	0.227 7(7)	0.602 1(4)	0.591 6(3)		C(52)	0.500 7(8)	0.748 2(9)	0.303 3(4)
C(2d)	0.390 2(7)	0.627 9(4)	0.652 0(4)		C(53)	0.568(1)	0.746(1)	0.221 3(6)
C(3d)	0.453(1)	0.573 1(8)	0.745 3(7)	0.740	C(54)	0.459(2)	0.775 1(7)	0.137 7(7)
C(3d′)	0.489(4)	0.595(2)	0.751(2)	0.260	C(55)	0.282(2)	0.805 0(8)	0.134 5(6)
C(4d)	0.320 8(8)	0.577 3(5)	0.809 7(4)		C(56)	0.209(1)	0.806 1(6)	0.216 3(5)
C(5d)	0.176 0(7)	0.661 7(4)	0.788 1(3)		C(60)	−0.085 7(8)	0.877 4(5)	0.843 7(4)
C(6d)	0.009 7(7)	0.648 4(4)	0.726 4(4)		C(61)	0.021 1(7)	0.962 0(5)	0.901 8(4)
C(7d)	−0.047(1)	0.554 2(6)	0.669 6(5)	0.840	C(62)	0.209 0(8)	0.973 2(5)	0.908 4(4)
C(7d′)	0.018(8)	0.524(5)	0.683(4)	0.160	C(63)	0.306(1)	1.052 8(6)	0.960 7(5)
C(8d)	0.103(1)	0.516 8(5)	0.615 8(6)	0.840	C(64)	0.219(1)	1.119 5(7)	1.009 1(6)
C(8d′)	0.059(7)	0.511(4)	0.578(4)	0.160	C(65)	0.037(1)	1.108 7(8)	1.005 8(7)
C(22)	−0.123 1(6)	0.894 4(4)	0.736 1(4)		C(66)	−0.063(1)	1.030 3(7)	0.952 3(5)
C(23)	−0.189 6(7)	1.003 2(5)	0.707 8(4)					

Table 2 Selected bond distances (Å) and angles (°) for complex **2**

Ru–Cl(1)	2.448(2)	Ru–Cl(2)	2.431(2)
Ru–N(21)	2.166(4)	Ru–N(31)	2.160(4)
Ru–C(1d)	2.212(5)	Ru–C(2d)	2.223(5)
Ru–C(5d)	2.202(5)	Ru–C(6d)	2.206(5)
N(21)–C(25)	1.278(7)	N(31)–C(35)	1.294(6)
C(25)–C(30)	1.461(7)	C(30)–C(35)	1.484(7)
Cl(1)–Ru–Cl(2)	160.1(1)	N(21)–Ru–N(31)	87.5(2)
Cl(1)–Ru–N(21)	80.9(1)	Cl(1)–Ru–N(31)	83.8(1)
Cl(2)–Ru–N(21)	84.4(1)	Cl(2)–Ru–N(31)	82.2(1)
C(1d)–Ru–C(6d)	79.7(2)	C(2d)–Ru–C(5d)	78.4(2)
Ru–N(21)–C(25)	123.1(3)	Ru–N(31)–C(35)	122.0(3)
N(21)–C(25)–C(30)	128.6(5)	N(31)–C(35)–C(30)	128.8(4)
C(25)–C(30)–C(35)	117.0(4)		

more time nearer the chloride than the other. The Ru–Cl distances, 2.448(2) and 2.431(2) Å, are in the expected range. For example, both the equivalent bond lengths in the starting material **1** are 2.437 Å.[20] The Ru–N distances [2.160(4) and 2.166(4) Å] are comparable to those observed in the pyridine complex [RuH(Cl)(py)$_2$(cod)] [2.153(2) and 2.167(2) Å].[22] These are longer than those found in typical [Ru(diimine)$_3$]$^{2+}$ complexes (normal range Ru–N 2.03–2.09 Å) the cationic nature of which leads to Ru–N bond contraction (for a recent example see ref. 23). The Ru–C distances at 2.212(5), 2.223(5), 2.202(5) and 2.206(5) Å are similar to those seen in other crystallographically characterised ruthenium η^4-cyclooctadiene complexes.[24–26]

The reactions of L^2 and L^3 with complex **1** lead to the analogous ruthenium complexes **3** and **4** which are isostructural with **2** according to NMR spectroscopic studies. Although these spectra indicate that **3** is substantially pure we were unable to obtain an acceptable elemental analysis of this complex. The reaction mixture has a tendency to turn green, empirically associated with oxidation to ruthenium(III), resulting in lower yields and paramagnetic impurities. One possible explanation for these observations is that there is a larger kinetic barrier towards co-ordination of L^2 than with L^1. The resulting slower reaction may result in oxidation of the labile *cis*-'RuCl$_2$(cod)' fragment before chloride isomerisation and bis(dihydrooxazole) co-ordination. These ideas are supported by the behaviour of the related L^3, reaction with complex **1** being even slower than for L^2. Monitoring the reaction by ^{1}H NMR spectroscopy in $CDCl_3$ indicates that formation of **4** (Scheme 2) requires over 100 h at room temperature. This retarded rate of complexation

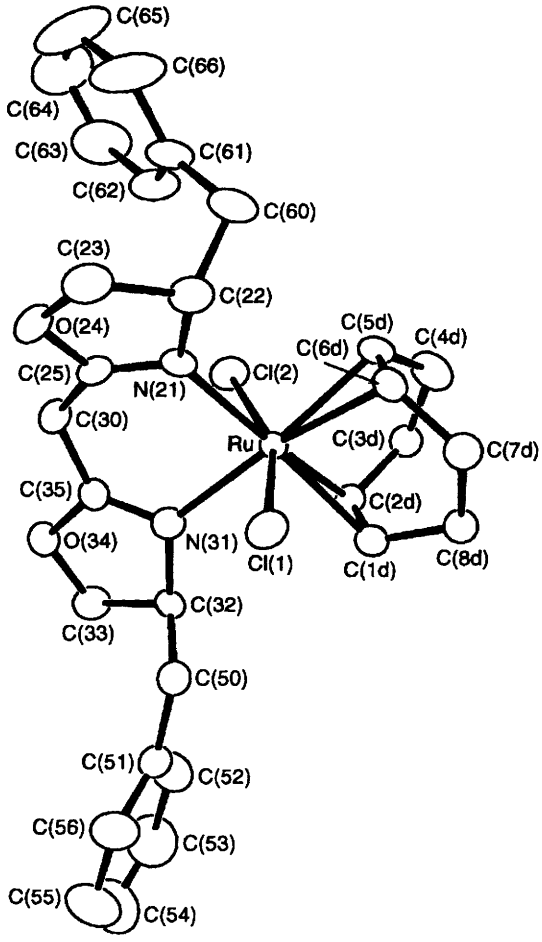

Fig. 1 Molecular structure of compound **2** including the atom numbering scheme; hydrogen atoms are omitted for clarity

for L^3 compared to L^2 may be explained by increased steric interactions between the isopropyl substituents of the approaching L^3 and the *cis*-'RuCl$_2$(cod)' generated by MeCN loss from **1**. The isopropyl substituents in L^3 have less opportunity to fold away from poor steric interactions than do the substituents in L^1 and L^2 due to the additional CMe_2 functions. Nevertheless, despite these kinetic barriers **4** is formed and is isolated in good yield as a single product with the expected spectroscopic

properties. In dilute solution it shows some tendency to dissociate the bis(dihydrooxazole) ligand. Recrystallisation of the complex occasionally results in poor recovery while the free bis(dihydrooxazole) can be detected in the mother-liquors. The imine stretch of complex **4** [ν_{CN}(KBr) 1623 cm^{-1}] is at distinctly lower energy than that of **3** [ν_{CN}(KBr) 1675 cm^{-1}] indicating C–N elongation and suggesting a similar ligand distortion to that shown in the crystal structure of **7** (see later).

Tungsten Complexes.—As we proposed to use L^3 for *in situ* addition to high-oxidation-state ruthenium centres it became apparent that we should investigate further its behaviour to determine whether the slow rate of complexation to **1** was due *only* to kinetic factors and not due to fundamental thermodynamic instability for complexes of this type. The slow ruthenium complexation by L^3 and its apparent loss in dilute solution suggest weakening of the metal–nitrogen bonds. As the electronic properties of L^2 and L^3 should be similar, differences in the steric demand of the two species should be reflected in lengthening of the metal–nitrogen bonds. Regrettably, the ruthenium complexes **3** and **4** proved non-crystalline and this led us to look at metal–nitrogen bond lengths in tungsten tetracarbonyl adducts as convenient stable model systems. Reaction of $[W(CO)_6]$ with the bis(dihydrooxazoles) ligands L^1–L^3 in tetralin leads to the tetracarbonyls **5**–**7** in 7–58% yield (Scheme 2). The lowest yield is associated with the hexamethyl oxazole L^3. Fortuitously, while the benzyl-derived complex **5** is an insoluble powder, the isopropyl derivatives **6** and **7** are crystalline allowing probing of the effects of the extra methyl groups on the co-ordination of bis(dihydrooxazoles). Views of the two tetracarbonyl complexes are shown in Figs. 2 and 3. Compound **6** crystallises as two independent molecules, but only one of these is shown. The fractional atomic coordinates for the two structures are shown in Tables 3 and 4. Selected bond lengths and angles for the two independent molecules of **6** are in Table 5; the equivalent values for compound **7** are displayed in Table 6 to aid comparisons.

It is apparent from the crystallographic data that substitution of the three methylene groups in L^2 with CMe_2 units renders L^3 a stronger σ donor. The shortening of the average W–N (0.07 Å, *ca.* 3% contraction) and W–C (0.14 Å, *ca.* 7% contraction) bond lengths are indicative of such behaviour. Introduction of the CMe_2 fragments into the dihydrooxazole rings results in deformation from an essentially planar ring to an envelope conformation. In addition a number of significant bond distortions result; for clarity these are shown highly exaggerated in structure **A**. Corey and Ishihara[18] suggest that dimethyl units at C(5) in these ligands cause the C(4) dihydrooxazole substituent to orient towards the metal in such complexes avoiding *gauche*-like interactions, as in structure **B**. However, the torsional angles in the four rings of the two independent molecules of **6** (φ_1 = 50.3, 54.0, 58.8, 60.0°; φ_2 = 64.6, 68.7, 69.5, 74.6°) are similar to those observed for **7** (φ_1 = 43.5, 60.9; φ_2 = 71.0, 79.4°), indicating only slight perturbation of the isopropyl twists in the solid state. Exclusion of solution-state extrapolations and crystal-packing effects may account for these observations, alternatively Corey's *gauche* effect is not applicable to these Pr^i-substituted oxazoles and their complexes.

We conclude that the slower complexation of L^3 by bulky metal fragments is solely a kinetic phenomenon encountered with bulky metal centres and that L^3 is a strong electron-rich donor well able to co-ordinate electron-deficient fragments, provided these are sterically non-demanding, such as RuO_2.

Aldehyde-promoted Epoxidations.—Distilled styrene is easily oxidised to its epoxide and benzaldehyde under Mukaiyama conditions,[2] even in the absence of metal catalysts.[14] Under such conditions successful asymmetric epoxidation will only be attained if: (*i*) the rate of catalysed epoxidation is competitive with underlying uncatalysed reactions, and (*ii*) the epoxidation

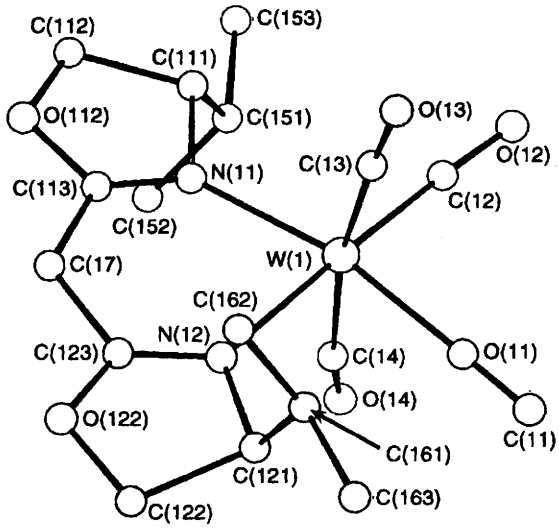

Fig. 2 Molecular structure of one of the two independent molecules of compound **6** including the atom numbering scheme; hydrogen atoms are omitted for clarity

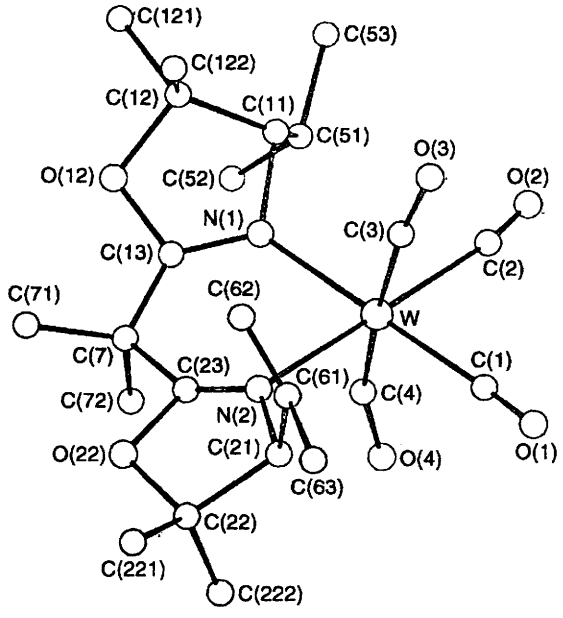

Fig. 3 Molecular structure of compound **7** including the atom numbering scheme; hydrogen atoms are omitted for clarity

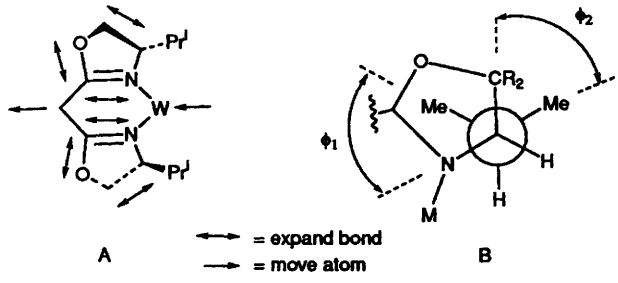

step is metal centred. It is instructive therefore to compare qualitative and quantitative rate differences between metal-free and -promoted reactions. Uncatalysed reactions of styrene (1.00 mol dm^{-3} in light-shielded Pr^iCHO) under O_2 (1 atm) at 40 °C are conveniently monitored by GC of the styrene consumption. A styrene concentration-independent rate constant k_0 = 1.22(3) × 10^{-5} dm^3 mol^{-1} was obtained. Equivalent reactions catalysed by $[Fe(acac)_3]$ (0.01 mol dm^{-3}) are about five times faster. These suffer slightly from reproducibility problems, but

Table 3 Final atomic coordinates for complex **6**

Atom	*x*	*y*	*z*
W(1)	−0.012 53(9)	0	−0.111 20(8)
N(11)	−0.273 0(10)	−0.029 3(6)	−0.103 8(10)
N(12)	−0.115 5(12)	0.036 4(6)	−0.303 5(10)
C(11)	0.198 0(12)	0.040 0(7)	−0.131 7(14)
O(11)	0.317 5(12)	0.062 0(6)	−0.141 5(12)
C(12)	0.072 1(16)	−0.026 3(8)	0.058 7(11)
O(12)	0.139 4(14)	−0.046 5(8)	0.150 4(11)
C(13)	0.078 1(15)	−0.067 4(5)	−0.201 6(14)
O(13)	0.137 3(14)	−0.106 0(5)	−0.235 2(14)
C(14)	−0.067 7(17)	0.070 2(5)	−0.010 0(15)
O(14)	−0.093 5(16)	0.105 4(6)	0.060 7(15)
W(2)	−0.491 92(10)	−0.251 89(5)	−0.584 35(8)
N(21)	−0.745 5(10)	−0.213 3(6)	−0.611 3(10)
N(22)	−0.598 6(12)	−0.277 8(6)	−0.393 7(9)
C(21)	−0.266 7(11)	−0.281 0(8)	−0.555 3(15)
O(21)	−0.143 7(12)	−0.298 9(8)	−0.532 8(13)
C(22)	−0.421 6(15)	−0.217 2(7)	−0.745 7(10)
O(22)	−0.372 3(15)	−0.200 8(7)	−0.845 7(10)
C(23)	−0.411 4(16)	−0.177 7(5)	−0.501 1(15)
O(23)	−0.356 3(16)	−0.138 0(6)	−0.455 5(14)
C(24)	−0.550 6(16)	−0.320 5(5)	−0.689 7(15)
O(24)	−0.580 0(16)	−0.358 6(5)	−0.748 1(14)
O(122)	−0.290 8(13)	0.059 0(7)	−0.478 9(11)
O(112)	−0.521 2(12)	−0.058 4(6)	−0.167 4(12)
O(222)	−0.764 9(14)	−0.290 6(6)	−0.234 9(11)
O(212)	−0.995 4(12)	−0.176 5(6)	−0.566 7(11)
C(122)	−0.148 3(14)	0.092 2(8)	−0.498 4(15)
C(112)	−0.489 1(15)	−0.085 7(8)	−0.047 8(13)
C(222)	−0.640 6(14)	−0.331 0(8)	−0.200 1(14)
C(212)	−0.974 3(14)	−0.161 6(8)	−0.698 0(12)
C(123)	−0.255 8(13)	0.033 4(8)	−0.363 3(12)
C(113)	−0.385 3(13)	−0.028 9(7)	−0.191 9(11)
C(223)	−0.733 9(13)	−0.265 1(6)	−0.347 8(12)
C(213)	−0.855 3(13)	−0.204 4(8)	−0.533 1(11)
C(17)	−0.395 0(15)	−0.001 0(8)	−0.321 9(12)
C(121)	−0.011 9(13)	0.068 2(6)	−0.397 1(12)
C(161)	0.108 2(15)	0.030 4(6)	−0.467 7(14)
C(162)	0.033 0(17)	−0.017 9(7)	−0.539 3(16)
C(163)	0.226 0(16)	0.062 9(9)	−0.547 9(15)
C(111)	−0.324 6(14)	−0.062 3(6)	0.009 9(10)
C(151)	−0.330 6(16)	−0.026 2(6)	0.137 7(12)
C(152)	−0.449 5(16)	0.021 0(7)	0.120 1(15)
C(153)	−0.373 6(16)	−0.062 7(8)	0.252 4(14)
C(27)	−0.854 1(16)	−0.222 6(7)	−0.394 3(12)
C(221)	−0.506 3(13)	−0.317 8(7)	−0.302 0(12)
C(261)	−0.354 3(15)	−0.290 5(7)	−0.231 5(15)
C(262)	−0.396 7(18)	−0.237 2(8)	−0.169 3(17)
C(263)	−0.259 7(17)	−0.330 7(9)	−0.141 7(16)
C(211)	−0.811 9(14)	−0.187 4(7)	−0.736 9(11)
C(251)	−0.833 8(16)	−0.229 2(6)	−0.853 8(12)
C(252)	−0.947 4(16)	−0.275 7(7)	−0.823 1(15)
C(253)	−0.896 6(17)	−0.196 3(9)	−0.974 1(14)

Table 4 Final atomic coordinates for complex **7**

Atom	*x*	*y*	*z*
W	0.0142(1)	0.0705(1)	0.0785(3)
O(12)	0.1797(11)	0.1843(10)	0.3990(34)
O(22)	−0.0896(12)	0.1659(11)	0.5024(33)
N(1)	0.1121(9)	0.1296(9)	0.1934(28)
N(2)	−0.0488(12)	0.0968(11)	0.2972(18)
C(1)	−0.0701(15)	0.0172(17)	0.0025(41)
O(1)	−0.1220(12)	−0.0253(12)	−0.0430(34)
C(2)	0.0720(15)	0.0544(16)	−0.0990(21)
O(2)	0.1046(15)	0.0428(14)	−0.2255(20)
C(3)	0.0591(16)	−0.0203(9)	0.1383(39)
O(3)	0.0889(13)	−0.0739(8)	0.1690(31)
C(4)	−0.0332(21)	0.1534(13)	−0.0169(40)
O(4)	−0.0721(15)	0.1937(14)	−0.0848(35)
C(11)	0.2014(17)	0.1200(17)	0.1608(39)
C(51)	0.2212(18)	0.1652(17)	0.0270(41)
C(52)	0.2091(20)	0.2447(18)	0.0377(39)
C(53)	0.3048(24)	0.1499(25)	−0.0593(45)
C(12)	0.2384(19)	0.1314(17)	0.3304(40)
C(121)	0.3209(18)	0.1663(18)	0.3523(40)
C(122)	0.2342(16)	0.0681(16)	0.4330(38)
C(13)	0.1077(17)	0.1678(16)	0.3272(4)
C(21)	−0.1233(18)	0.0620(17)	0.3505(39)
C(61)	−0.1026(18)	−0.0103(17)	0.4226(44)
C(62)	−0.0365(23)	−0.0174(22)	0.5236(44)
C(63)	−0.1726(24)	−0.0570(23)	0.4687(43)
C(22)	−0.1616(17)	0.1231(16)	0.4654(41)
C(221)	−0.1998(24)	0.0944(22)	0.6251(42)
C(222)	−0.2166(20)	0.1602(19)	0.3593(40)
C(23)	−0.0335(17)	0.1512(16)	0.3810(42)
C(7)	0.0343(14)	0.2019(14)	0.4022(43)
C(71)	0.0543(17)	0.2231(17)	0.5627(40)
C(72)	0.0074(17)	0.2697(13)	0.2975(40)

usable data can be obtained with persistence. The catalysed reactions best fit an apparent pseudo-first-order rate constant $k_1 = 6.68(5) \times 10^{-5}$ s^{-1}. Light sources are known to benefit aldehyde-driven epoxidations and we suspect fortuitous light during GC sample removal and other adventitious radical initiators as the cause of the reproducibility errors. Early workers obtained comparable rates (10^{-6}–10^{-4} dm^3 mol^{-1}) for

Table 5 Selected bond distances (Å) and angles (°) for complex **6**; n = 1 for molecule 1, 2 for molecule 2

	Molecule 1	Molecule 2
W(*n*)–C(*n*1)	1.995(8)	1.977(7)
W(*n*)–C(*n*2)	1.928(8)	1.953(8)
W(*n*)–C(*n*3)	2.034(8)	2.078(8)
W(*n*)–C(*n*4)	2.050(8)	2.119(8)
W(*n*)–N(*n*1)	2.247(7)	2.274(7)
W(*n*)–N(*n*2)	2.258(8)	2.253(8)
N(*n*1)–C(*n*13)	1.244(8)	1.248(8)
N(*n*2)–C(*n*23)	1.268(8)	1.261(8)
C(*n*7)–C(*n*13)	1.478(9)	1.474(9)
C(*n*7)–C(*n*23)	1.489(9)	1.482(9)
C(*n*11)–C(*n*12)	1.542(9)	1.538(9)
C(*n*21)–C(*n*22)	1.582(9)	1.581(9)
C(*n*13)–O(*n*12)	1.355(9)	1.357(9)
C(*n*23)–O(*n*22)	1.342(9)	1.340(9)
C(*n*1)–W(*n*)–C(*n*2)	89.2(6)	87.9(6)
C(*n*3)–W(*n*)–C(*n*4)	171.3(5)	171.1(6)
N(*n*1)–W(*n*)–N(*n*2)	81.3(4)	79.9(4)
W(*n*)–N(*n*1)–C(*n*13)	129.4(8)	132.5(8)
W(*n*)–N(*n*2)–C(*n*23)	132.3(8)	129.6(8)
N(*n*1)–C(*n*13)–C(*n*7)	130(1)	126(1)
N(*n*2)–C(*n*23)–C(*n*7)	125(1)	129(1)
C(*n*13)–C(*n*7)–C(*n*23)	120(1)	119(1)

Table 6 Selected bond distances (Å) and angles (°) for complex **7**

W–C(1)	1.835(9)	W–C(2)	1.828(9)
W–C(3)	1.921(9)	W–C(4)	1.922(9)
W–N(1)	2.187(9)	W–N(2)	2.192(9)
N(1)–C(13)	1.35(4)	N(2)–C(23)	1.27(3)
C(7)–C(13)	1.51(4)	C(7)–C(23)	1.48(4)
C(11)–C(12)	1.59(4)	C(21)–C(22)	1.64(4)
C(13)–O(12)	1.37(3)	C(23)–O(22)	1.42(4)
C(1)–W–C(2)	90(1)	C(3)–W–C(4)	169(2)
N(1)–W–N(2)	81.8(9)	W–N(1)–C(13)	127(2)
W–N(2)–C(23)	124(2)	N(1)–C(13)–C(7)	129(3)
N(2)–C(23)–C(7)	137(3)	C(13)–C(7)–C(23)	106(2)

Table 7 Oxidation studies of styrene and *cis*-*trans*-stilbene [a]

Alkene	Catalyst (mol %)	Oxidant	T/°C	Radical suppression [b]	t [c]/h	Yield (%) Epoxide	Yield (%) PhCHO
Styrene	—	$Pr^iCHO–O_2$	22	No	3 [d]	58	38
	—	$Pr^iCHO–O_2$	22	Yes	> 20 [e]	14	14
	1 (1)	$Pr^iCHO–O_2$	22	No	4.5	38	20
	1 (1)	$Pr^iCHO–O_2$	22	Yes	7	32	20
	1 (1) + L^3 (4)	$Pr^iCHO–O_2$	22	No	2.2	57	14
	1 (1) + L^3 (4)	$Pr^iCHO–O_2$	22	Yes	4.3	40	25
	aibn (1)	$Pr^iCHO–O_2$	22	No	72	25	48
	aibn (1)	$Pr^iCHO–O_2$	22	Yes	72	31	53
	2 (1)	$Pr^iCHO–O_2$	22	No	2	61	16
	3 (1)	$Pr^iCHO–O_2$	22	No	6.3	45	15
	4 (1)	$Pr^iCHO–O_2$	22	No	2	50	4
trans-Stilbene	—	$Pr^iCHO–O_2$	22	No	10	80	19
	1 (1)	$Pr^iCHO–O_2$	22	No	4	96	2
cis-Stilbene	—	$Pr^iCHO–O_2$	22	No	> 23.5 [f]	30 (*trans*), 12 (*cis*)	—
	1 (1)	$Pr^iCHO–O_2$	22	No	9.5	30 (*trans*), 16 (*cis*)	—
Styrene	**1** (1) + L^3 (4)	Bu^tO_2H	0	No	26 [g]	8	34
trans-Stilbene	**1** (1) + L^3 (4)	$NaIO_4$	10	No	8.5	50	—

[a] Reaction conditions: alkene, 1.31 mmol; oxidant, 6.50 mmol; 1,2-dichloroethane, 2 cm^3. Only epoxide and PhCHO yields were determined. [b] 50 ppm 4-*tert*-butylcatechol if added. [c] For 95% conversion. [d] Reaction requires > 30 h on a 13.1 mmol scale. [e] Conversion 28% at 20 h. [f] Conversion 57% at 23.5 h. [g] 70% conversion.

aliphatic aldehyde autooxidations to peracids, and also noted reproducibility problems.[27,28] Styrene and stilbene epoxidation studies using complexes **1**–**4**, **1** in the presence of an excess of L^3, and azoisobutyronitrile (aibn) promoters offer useful probes for radical intervention and insights into whether the epoxidation is metal centred or not (Table 7). Obtaining rate data in the 1,2-dichloroethane solvent used for these reactions is problematic; only qualitative comparison of the reactions proved possible by determining the time required for conversion of > 95% styrene by GC analysis. The uncatalysed reactions demonstrate variable induction periods depending on the reaction scale. These periods are insignificant on 1 mmol scales but increase to more than 10 h on ten times this scale. Within the induction period only traces of peracid (< 0.02 mol dm^{-3}) may be detected titrimetrically but this concentration increases steadily as epoxidation commences. The highest level of peracid we have detected in the uncatalysed reactions is *ca.* 0.1 mol dm^{-3}. These observations are consistent with peracid generation by aldehyde autooxidation. A radical chain-based mechanism is also supported by inhibition of 1 mmol scale reactions by 4-*tert*-butylcatechol. In the presence of this radical trap styrene oxidation is initially completely inhibited but recommences after some 20 h, presumably once the inhibitor is exhausted. Uncatalysed epoxidation of *trans*-stilbene is stereospecific but *cis*-stilbene leads mostly to the *trans* epoxide.

The metal-promoted reactions result in rapid alkene oxidation, while aibn gives mostly slow C–C bond cleavage. Complexes **1**–**4** and **1** in the presence of L^3 all show similar behaviour: within experimental error all the styrene reactions lead to the corresponding racemic oxide suggesting that the oxidation is not metal centred and that aldehyde autooxidation-derived peracid is also responsible for the oxidation. However, little free peracid can be detected titrimetrically in these metal-promoted reactions, $[RCO_3H]_{max} < 0.06$ mol dm^{-3}.

Aliphatic aldehydes react thermally (rapidly above 0 °C), photochemically (280–360 nm light), or with radical initiators to yield peracyl radicals, $RCO_3^{\bullet}$, in the presence of O_2.[27] Chain propagation proceeds through CH abstraction of a second aldehyde molecule by $RCO_3^{\bullet}$ yielding peracids, RCO_3H and $RCO^{\bullet}$ with rate k_{prop}.[29] The latter rapidly captures O_2 regenerating $RCO_3^{\bullet}$. The question arises whether it is $RCO_3^{\bullet}$ or RCO_3H which epoxidises the alkene. Although alkenes are known to add $RCO_3^{\bullet}$ in the gas phase,[30] comparison of literature rates, corrected to common temperature, indicate that k_{prop} is faster than alkene addition by $RCO_3^{\bullet}$ (ring closure to the oxirane is known to be rapid[30]), provided: (*i*) electron-poor alkenes are involved, and (*ii*) the ratio [RCHO]:[alkene] is high.[28,30] However, the reaction of $RCO_3^{\bullet}$ with 1,2-disubstituted alkenes results in a loss of (*E*/*Z*) stereospecificity and this may account for the behaviour of *cis*-stilbene in these epoxidations. As we are able to detect peracids *via* iodometric titration in our reactions it seems the best description of these reactions is that in Scheme 3.

Although most of our ruthenium species are excellent promoters of cycle 1, the generation of racemic styrene oxide is indicative of poor performance in cycle 2. Either the formation of oxoruthenium species is inhibited with respect to epoxidation by even low levels of free Pr^iCO_3H, or the oxo species once formed show poor enantioselectivity. In attempts to address this question, complex **1** in the presence of an excess of L^3 was used as a catalyst for the epoxidation of styrene or *trans*-stilbene using terminal oxidants other than $Pr^iCHO–O_2$ (Table 7). Unfortunately, the oxides produced in these reactions are also racemic within the error of measurement indicating that L^3 is a rather poor ligand. It is suspected that one reason for this behaviour is the inability of the ruthenium centre easily to co-ordinate two molecules of L^3, as species of the kind $[Ru(=O)L(N–N)_2]^{2+}$ (L = solvent or water, N–N is a bidentate ligand with two nitrogen donors) are believed to be the active centres in these reactions.[31] In fact a recent study using slightly less-encumbered ligands than L^1–L^3 met with some success, enantioselectivities of 6–21% being realised.[32]

Conclusion

Although appropriate ruthenium pre-catalysts **2**–**4** are easily prepared, the preparation of chiral epoxides using these catalysts is not feasible with aliphatic aldehydes in the presence of molecular oxygen. Major problems are epoxidations carried out by free peroxy radicals and peracids generated by aldehyde autooxidation. Ruthenium-centred asymmetric epoxidation does not compete in either rate or selectivity. Although two successful approaches to aerobic asymmetric epoxidation using aldehydes have recently been reported we note that these are restricted to dihydronaphthalene epoxidation and other alkenes which are rather resistant to epoxidation by free peracids.[5,6] We are currently engaged in the search for new catalysts and conditions which will allow for chiral

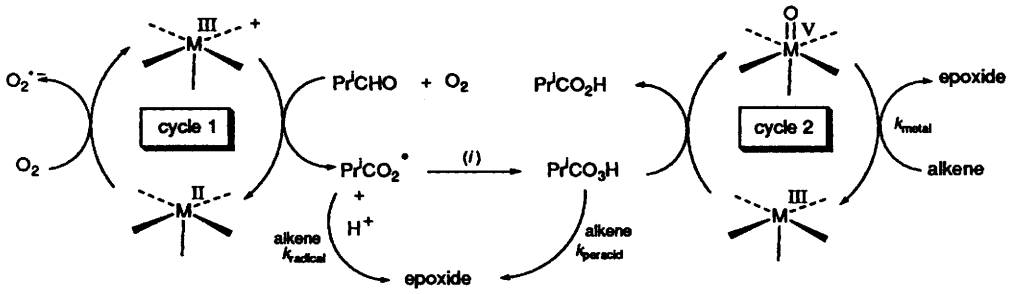

Scheme 3 (*i*) Autocatalysis, Pr^iCHO–O_2

epoxidation of a wide range of alkenes using radical-derived O-atom donors.

Experimental

General.—All manipulations, except oxidations and routine organic preparations, were carried out under nitrogen atmospheres using standard Schlenk techniques. All alkenes and Pr^iCHO were commercial products (Aldrich) distilled and stored under nitrogen at −20 °C over A4 molecular sieves. Dichloromethane was distilled from CaH_2 immediately prior to use; hexane, light petroleum (b.p. 40–60 °C) and Et_2O were dried over sodium wire. Tetrahydrofuran was distilled from sodium–benzophenone. All other reagents were used as supplied. Column chromatography and preparative TLC were run on activated silica gel, Rhône-Poulenc Sorbsil C60 40/60H and Merck Kieselgel 60 $HF_{254+366}$ respectively. Columns run on alumina used Bockmann grade I material deactivated 5% w/w with concentrated ammonia solutions. Infrared spectra were recorded using a Perkin-Elmer 983G instrument, proton NMR spectra on a JEOL-270 (270 MHz) or Bruker AM-500 (500 MHz) spectrometers, carbon-13 (67.8 MHz) NMR spectra on the JEOL-270 and mass spectra on Finnigan 1020 (electron-impact ionisation, EI) or VG-ZAB (fast atom bombardment ionisation, FAB) machines (relative peak intensities normalised to 100%). Catalytic runs were monitored using a Perkin-Elmer 8320 gas chromatograph equipped with a 24 m capillary BP-20 column. Optical activities were assayed by polarimetry on an Optical Activity AA-10 instrument, by chiral ^1H NMR shift reagents, or GC analysis on a 24 m Cyclodex-B column as appropriate. Optical rotation studies were conducted at ambient temperature with concentration measured in g per 100 cm^3 solution.

The bis(dihydrooxazoles) L^1 and L^2 were prepared as previously described.[16] The simple valine derivatives **I**, **III** and **V** were obtained by routine organic chemistry: **I**, R_f 0.80 (CH_2Cl_2–Et_2O, 4:1), ^1H NMR (270 MHz, $CDCl_3$) δ_H 7.05 (1 H, s, NH), 4.60 (1 H, m, J = 8.5, 5.0, 4.5, CHN), 3.80 (3 H, s, OMe), 2.27 (1 H, double spt, J = 6.0, 5.0, C*H*Me_2), 0.98 (3 H, d, J = 6.0, CH*Me*$_2$) and 0.95 (3 H, d, J = 6.0, CH*Me*$_2$); **III**, R_f 0.65, ^1H NMR δ_H 6.80 (1 H, br s, NH), 3.80 (1 H, dd, J = 10.0, 3.0, CHN), 2.23 (1 H, m, J = 6.0, 5.0, 3.0, C*H*Me_2), 1.90 (1 H, br s, OH), 1.35 (3 H, s, MeC^2), 1.25 (3 H, s, MeC^2), 0.97 (3 H, d, J = 6.0, CH*Me*$_2$) and 0.93 (3 H, d, J = 6.0, CH*Me*$_2$); **V**, R_f 0.59, ^1H NMR δ_H 2.44 (1 H, d, J = 3.0, HC^3), 1.95 (1 H, m, J = 7.0, 3.0, C*H*Me_2), 1.25 (3 H, s, MeC^2), 1.15 (3 H, s, MeC^2), 1.00 (3 H, d, J = 7.0, MeC^4) and 0.90 (3 H, d, J = 7 Hz, MeC^4). The amino and hydroxy functions were only apparent as a broad signal at *ca.* δ_H 2.0. (See SUP 57057 for full details.)

N,N′-*Bis*[(1S)-1-(*methoxycarbonyl*)-2-*methylpropyl*]-2,2-*dimethylpropane*-1,3-*diamide* **V**.—To a solution of methyl L-valinate hydrogenchloride[33] (1.00 g, 5.90 mmol) and triethylamine (4.1 cm^3, 11.9 mmol) in CH_2Cl_2 (100 cm^3) at −78 °C was added dimethylmalonyl chloride (0.50 g, 2.98 mmol)[34] dropwise. The solution was allowed to come to room temperature and then stirred (20 h). Standard work-up yielded the diamide as a colourless solid in quantitative yield which was recrystallised from CH_2Cl_2–hexane, R_f 0.70 (MeOH–CH_2Cl_2, 1:9), m.p. 90–94 °C (Found: C, 56.9; H, 8.3; N, 7.6. $C_{17}H_{30}N_2O_6$ requires C, 57.0; H, 8.4; N, 7.8%); ν_{max} 3300s, 2960w, 1738s, 1636s, 1622m, 1462w, 1431w, 1305w and 1198w cm^{-1}. NMR ($CDCl_3$): ^1H (270 MHz), δ_H 7.05 (2 H, br d, J = 8.5, NH), 4.51 (2 H, dd, J = 8.5, 5.0, CHN), 3.74 (6 H, s, OMe), 2.19 (2 H, double spt, J = 6.8, 5.0, C*H*Me_2), 1.52 (6 H, s, central CMe_2), 0.93 (6 H, d, J = 6.8, CH*Me*$_2$) and 0.90 (6 H, d, J = 6.8 Hz, CH*Me*$_2$); ^{13}C (67.8 MHz), δ_C 173.6 (CO), 172.2 (CO), 67.6 (CHN), 52.2 (OMe), 49.6 (central CH_2), 31.0 (*C*HMe_2), 24.0 (C*Me*$_2$), 19.1 and 17.8 (CH*Me*$_2$). EI mass spectrum: m/z 358 (1, M^+), 299 (42), 228 (35), 201 (19), 168 (19), 130 (26), 98 (26) and 70 (100%). α(589.3 nm, 0.95, in $CHCl_3$) = −117°.

N,N′-*Bis*[(3S)-2-*hydroxy*-2,4-*dimethylpent*-3-*yl*]-2,2-*dimethylpropane*-1,3-*diamide* **VI**.—*Method* 1. To a solution of (*S*)-3-amino-2,4-dimethylpentan-2-ol **IV** (3.7 g, 28.3 mmol) and triethylamine (5.7 g, 56.8 mmol) in CH_2Cl_2 (250 cm^3) at −78 °C was added dimethylmalonyl chloride (2.39 g, 14.2 mmol)[34] dropwise. The solution was allowed to warm to −5 °C (1 h). Extraction with CH_2Cl_2, washing (ice–water), drying (Na_2SO_4) and evaporation under vacuum yielded the diamine (4.70 g, 46%) as a white solid which was recrystallised from CH_2Cl_2–hexane, R_f 0.66 (CH_2Cl_2–MeOH, 9:1), m.p. 133–134 °C (Found: C, 63.7; H, 10.8; N, 7.75. $C_{19}H_{38}N_2O_4$ requires C, 63.65; H, 10.7; N, 7.8%); ν_{max} 3445s, 2970m, 2940w, 1640s, 1500m, 1400w, 1380w and 1180 cm^{-1}. NMR ($CDCl_3$): ^1H (270 MHz), δ_H 7.00 (2 H, br d, J = 10.0, NH), 3.80 (2 H, dd, J = 10.0, 3.0, CHN), 2.14 (2 H, double spt, J = 6.0, 3.0, C*H*Me_2), 2.00 (2 H, br s, OH), 1.57 (6 H, s, central CMe_2), 1.20 (6 H, s, HOC*Me*$_2$), 1.25 (6 H, s, HOC*Me*$_2$), 0.95 (6 H, d, J = 6.0, CH*Me*$_2$) and 0.90 (6 H, d, J = 6.0 Hz, CH*Me*$_2$); ^{13}C (67.8 MHz), δ_C 174.4 (CO), 73.6 (CHN), 60.7 (*C*Me_2), 49.9 (*C*Me_2), 29.1 (Me), 28.2 (*CH*Me_2), 26.6 (Me), 24.4 (Me), 22.4 (Me) and 16.9 (Me). EI mass spectrum: m/z 359 (M^+, 2) 299 (40), 282 (72), 183 (68), 140 (50), 115 (25), 45 (97) and 72 (100%). α(589.3 nm, 0.95, in $CHCl_3$) = −27.7°.

Method 2. A solution of LiMe (0.87 cm^3 of 1.5 mol dm^{-3} Et_2O solution, 1.31 mmol) was added to a solution of the diamide **V** (78 mg, 0.22 mmol) in thf (3 cm^3) at −78 °C. The solution was allowed to warm to room temperature and stirred (25 h). Acidification with aqueous HCl, extraction with dichloromethane and a standard work-up yielded compound **VI** (74 mg, 95%) with identical properties to that prepared by method 1.

2,2′-*Isopropylidenebis*[(4S)-4,5-*dihydro*-4-*isopropyl*-5,5-*dimethyloxazole*] L^3.—The diamide **VI** (1.33 g, 3.71 mmol) was refluxed in CH_2Cl_2 (30 cm^3) containing A4 molecular sieves (10 g) and $MeSO_3H$ (1.42 g, 14.86 mmol) for 2 h. Chromatography on Al_2O_3 (1% MeOH in CH_2Cl_2) yielded a white solid (0.63 g, 53%), R_f 0.71 (hexane–ethyl acetate, 5:2), m.p. 45–47 °C (Found: C, 70.5; H, 10.7; N, 8.6. $C_{19}H_{34}N_2O_2$ requires C, 70.8; H, 10.6; N, 8.7%); ν_{max}(KBr disc) 2980m, 2963m, 2950m, 2938m, 2865m, 2842m (CH), 1651s (CN), 1467m, 1451m, 1382m, 1365m, 1258m, 1110m and 1088m cm^{-1}. NMR ($CDCl_3$): ^1H (270 MHz), δ_H 3.30 (2 H, d, J = 6.6, CHN), 1.77

(2 H, oct, J = 6.6 CHMe$_2$), 1.45 (6 H, s, central CMe$_2$), 1.33 (6 H, s, Me$_2$C^5), 1.28 (6 H, s, Me$_2$C^5), 0.99 (6 H, d, J = 6.6, CHMe_2) and 0.98 (6 H, d, J = 6.6 Hz, CHMe_2); ^{13}C (67.80 MHz) δ_C 167.3 (CN), 86.2 (central CMe$_2$), 79.2 (CHN), 38.6 (Me$_2$C^5), 29.3, 23.9 (CHMe$_2$ + central CMe_2), 23.8, 21.4, 21.1 and 19.5 (CHMe_2 + Me_2C^5). EI mass spectrum: m/z 322 (20, M^+), 279 (85, M^+ − Pr^i), 183 (45), 167 (70), 138 (85), 125 (35), 96 (60), 68 (75), 55 (70) and 43 (100%). α(589.3 nm, 1.00, in $CHCl_3$) −107.0°. Attempted oxidative degradation of L^3 in the presence of 4 equivalents of NiO_2 in refluxing $CDCl_3$ (6 h) led to no reaction as assayed spectroscopically. No epimeric (*R*,*S*)-L^3 was apparent within the limit of ^{1}H NMR detection.

Reaction of [{RuCl$_2$(cod)}$_n$] *with the Anion of* L^1 *in the Presence of Air*.—Compound L^1 (0.60 g, 1.80 mmol) in thf (30 cm^3) was treated at −78 °C with LiBu (1.2 cm^3 of 1.6 mol dm^{-3} hexane solution, 1.9 mmol), stirred at this temperature (30 min) and then at room temperature (5 min). The reaction mixture was recooled to −78 °C and solid [{RuCl$_2$(cod)}$_n$] (0.30 g, 1.07 mmol) added against a counter flow of nitrogen. The brown suspension was allowed to warm to room temperature (1 h) and then refluxed (1 h) in the presence of limited amounts of air (*ca.* 1–5 mmol). The resulting blue solution was evaporated to a blue solid which was extracted with toluene and filtered through Celite. The extracts were concentrated and layered with hexane to yield a deep black-blue powder tentatively assigned as *dichlorobis*{2,2′-*methylenebis*[(4S)-4-*benzyl*-4,5-*dihydrooxazole*]}*ruthenium*(III) *chloride*, as a mono-toluene solvate (0.52 g, 50%), m.p. 154–156 °C (decomp.) (Found: C, 58.7; H, 5.5; N, 5.8. $C_{45.5}H_{48}Cl_3N_4O_4Ru$ requires C, 59.1; H, 5.45; N, 6.1%); ν_{max}(KBr disc) 3063w, 3030w, 2958w, 2925w (CH), 1592vs (CN), 1540vs, 1498s, 1453m, 1384w, 1222m, 1080m, 1030m, 744m, 730m and 702s cm^{-1}. ^{1}H NMR (270 MHz, $CDCl_3$): δ_H 7.37–7.14 (5 H, m, C_6H_5Me), 2.36 (3 H, s, C_6H_5Me); very broad signals due to co-ordinated L^1 appear over the range δ_H 0.5–8.0. FAB mass spectrum: m/z 767 (5, M^+ − 2Cl), 541 (45) and 435 (100%, M^+ − 2Cl − L^1). The complex proved too dark to give accurate polarimetry data. Attempts at rational preparation *via* rigorous air exclusion or direct combination of L^1 with $K_2[RuCl_5(OH_2)]$ led only to intractable mixtures.

trans-*Dichloro*(η^4-*cycloocta*-1,5-*diene*){2,2′-*methylenebis*-[(4S)-4-*benzyl*-4,5-*dihydrooxazole*]}*ruthenium*(II) **2**.—Solid [RuCl$_2$(NCMe)$_2$(cod)] **1**[35] (0.09 g, 0.25 mmol) was added to a solution of L^1 (0.25 g, 0.75 mmol) in CH_2Cl_2 (10 cm^3). The orange solution was stirred at room temperature for 6–7 h and then evaporated under reduced pressure. The oily solid was scratched with acetonitrile (2 cm^3) to yield *trans*-[RuCl$_2$(cod)-L^1] **2** as a yellow powder (0.06 g, 47%), m.p. 134–135 °C (decomp.) (Found: C, 56.3; H, 5.4; N, 4.4. $C_{29}H_{34}Cl_2N_2O_2Ru$ requires C, 56.7; H, 5.6; N, 4.55%); ν_{max}(KBr disc) 3055m, 3039m, 2970m, 2942m, 2910m, 2883m, 2839m (CH), 1670s (CN), 1443m, 1247m, 1234m, 1180m, 1016m, 715m and 706m; ($CHCl_3$) 1670s cm^{-1} (CN). NMR ($CDCl_3$): ^{1}H (500 MHz), δ_H 7.32–7.17 (10 H, m, Ph), 4.87 (2 H, m, =CH of cod), 4.49 (2 H, m, =CH of cod), 4.42 (2 H, m, CHN), 4.30 (2 H, dd, J = 8.7, 3.0, HC^5), 4.23 (2 H, t, J = 8.7, HC^5), 3.85 (2 H, s, central CH_2), 3.30 (2 H, dd, J = 14.2, 3.4, CH_2Ph), 2.86 (2 H, m, CH_2 of cod), 2.65 (2 H, m, CH_2 of cod), 2.59 (2 H, dd, J = 14.2, 10.2 Hz, CH_2Ph), 2.24 (2 H, m, CH_2 of cod) and 2.02 (2 H, m, CH_2 of cod); ^{13}C (67.80 MHz), δ_C 166.1 (CN), 136.4 (*ipso*-C of Ph), 129.4, 128.8 (*o*-, *m*-*C* of Ph), 127.0 (*p*-C of Ph), 90.5, 87.3 (=CH of cod), 73.0 (CHN), 66.0 (central CH_2), 39.7 (CH_2Ph), 30.2, 29.5 (CH_2 of cod) and 28.6 (C^5). FAB mass spectrum: m/z 614 (10, M^+), 579 (10, M^+ − Cl), 543 (100, M^+ − 2Cl) and 335 (60). α(589.3 nm, 0.08, in $CHCl_3$) +298°.

trans-*Dichloro*(η^4-*cycloocta*-1,5-*diene*){2,2′-*methylenebis*-[(4S)-4,5-*dihydro*-4-*isopropyloxazole*]}*ruthenium*(II) **3**.—This product was obtained in a similar manner to complex **2**, except that MeCN was used as a solvent, to yield a somewhat impure green-yellow powder (42%), m.p. 134 °C (Found: C, 46.7; H, 6.6; N, 5.3. $C_{21}H_{34}Cl_2N_2O_2Ru$ requires C, 48.65; H, 6.6; N, 5.4%); ν_{max}(KBr disc) 2957m, 2875m, 2828w (CH), 1675s (CN), 1434m, 1236m, 1173m and 1013s; (CH_2Cl_2) 1668m cm^{-1} (CN). NMR ($CDCl_3$): ^{1}H (270 MHz), δ_H 4.49 (2 H, m, =CH of cod), 4.32–4.17 (6 H, m, CHN + H^{5}C), 4.03 (2 H, m, =CH of cod), 3.84 (2 H, s, central CH_2), 2.73 (2 H, m, CH_2 of cod), 2.44 (2 H, m, CH_2 of cod), 2.17–2.00 (4 H, m, CH_2 of cod), 1.81 (2 H, m, CHMe$_2$), 0.76 (6 H, d, J = 7.0, CHMe_2) and 0.72 (6 H, d, J = 7.5 Hz, CHMe_2); ^{13}C (67.80 MHz), δ_C 165.1 (CN), 90.4, 86.8 (=CH of cod), 70.1 (CHN), 69.1 (central CH_2), 30.3, 29.3 (CH_2 of cod), 28.1 (C^5), 18.8 (CHMe_2) and 14.2 (CHMe_2); the isopropyl CH apparently overlaps with the signal at 29.3. FAB mass spectrum: m/z 518 (16, M^+), 447 (82, M^+ − 2Cl), 412 (60), 333 (18) and 239 (100%). Compound **3** proved too reactive in solution to allow accurate polarimetry results to be obtained.

trans-*Dichloro*(η^4-*cycloocta*-1,5-*diene*){2,2′-*isopropylidene-bis*[(4S)-4,5-*dihydro*-4-*isopropyl*-5,5-*dimethyloxazole*]}*ruthenium*(II) **4**.—Compound L^3 (0.10 g, 0.31 mmol) was added to ruthenium complex **1**[35] (0.11 g, 0.30 mmol) in dry CH_2Cl_2 (15 cm^3) and stirred (120 h) at ambient temperature. Evaporation under vacuum and prompt recrystallisation from CH_2Cl_2–hexane yielded complex **4** as orange crystals (99 mg, 55%), m.p. 131–132 °C (decomp.) (Found: C, 54.1; H, 7.75; N, 4.5. $C_{27}H_{46}Cl_2N_2O_2Ru$ requires C, 53.8; H, 7.7; N, 4.6%); ν_{max}(KBr disc) 2958m, 2928s, 2857m (CH), 1623s (CN), 1516m, 1465s, 1358m, 1301s, 1220m, 1086m and 1027m; ($CHCl_3$) 1625 m cm^{-1} (CN). ^{1}H NMR (270 MHz, $CDCl_3$): δ_H 4.56 (2 H, m, =CH of cod), 4.28 (2 H, m, =CH of cod), 3.45 (2 H, d, J = 3.0, CHN), 2.85 (2 H, m, CH_2 of cod), 2.42 (2 H, m, CH_2 of cod), 2.23 (4 H, m, CH_2 of cod), 1.78 (2 H, double spt, J = 7.5, 3.0, CHMe$_2$), 1.70 (6 H, s, central CMe$_2$), 1.59 (6 H, s, Me$_2$C^5), 1.58 (6 H, s, Me$_2$C^5), 0.99 (6 H, d, J = 7.5, CHMe$_2$) and 0.96 (6 H, d, J = 7.5 Hz, CHMe$_2$). FAB mass spectrum: m/z 529 (67, M^+ − 2Cl), 493 (100), 457 (28), 417 (35) and 323 (47%). α(589.3 nm, 0.41, in $CHCl_3$) +245°.

Tetracarbonyl{2,2′-*methylenebis*[(4S)-4-*benzyl*-4,5-*dihydro-oxazole*]}*tungsten*(0) **5**.—A suspension of [W(CO)$_6$] (0.50 g, 1.42 mmol) and L^1 (0.50 g, 1.50 mmol) in tetralin (15 cm^3) was heated to 190 °C during which time the [W(CO)$_6$] dissolved and CO evolution was noted. The yellow solution was stirred at this temperature for 0.5 h. On cooling to room temperature a large mass of yellow microcrystals formed which were filtered off and washed with $CHCl_3$ (3 × 5 cm^3) and hexane (2 × 5 cm^3), yielding 0.52 g (58%), m.p. 196–198 °C (decomp.) (Found: C, 47.9; H, 3.5; N, 4.6. $C_{25}H_{22}N_2O_6W$ requires C, 47.6; H, 3.5; N, 4.4%); ν_{max}(KBr disc) 3060vw, 2910w (CH), 2005m, 1875s, 1841s, 1803(sh), 1788s (CO) and 1660m (CN); (CH_2Cl_2) 2006m, 1876s, 1863s, 1815s (CO) and 1665 cm^{-1} (CN). ^{1}H NMR (270 MHz, CD_2Cl_2): δ_H 7.36–7.21 (10 H, m, Ph), 4.48–4.60 (2 H, m, HC^5), 4.26–4.34 (4 H, m, HC^5), 3.64 (4 H, dd, J = 13.0, 3.0, CH_2Ph), 3.41 (2 H, s, central CH_2) and 2.75 (4 H, dd, J = 13.0, 9.5 Hz, CH_2Ph). FAB mass spectrum: m/z 630 (3, M^+), 602 (4, M^+ − CO) and 161 (100%). The compound was too insoluble to allow accurate polarimetry studies.

Tetracarbonyl{2,2′-*methylenebis*[(4S)-4,5-*dihydro*-4-*isopropyloxazole*]}*tungsten*(0) **6**.— Prepared in the same manner as complex **5**. Product isolation was effected by filtration of the reaction mixture through Celite, concentration of the solution, addition of pentane and cooling. Yield 35%, m.p. 156–157 °C (decomp.) (Found: C, 38.3; H, 3.8; N, 5.1. $C_{17}H_{22}N_2O_6W$ requires C, 38.2; H, 4.15; N, 5.2%); ν_{max}(KBr disc) 2963w, 2924w, 2871vw, 2850vw (CH), 2003m, 1898(sh), 1890s, 1875s, 1851s, 1846(sh), 1804(sh), 1795s (CO) and 1681m (CN); (CH_2Cl_2) 2006m, 1876s, 1863(sh), 1815s (CO) and 1665 cm^{-1} (CN). ^{1}H NMR (270 MHz, $CDCl_3$): δ_H 4.46–4.16 (6 H, m, HC^4

Table 8 Crystal and X-ray structural analysis data for complexes **2**, **6** and **7**

	2	**6**	**7**
Empirical formula	$C_{29}H_{34}Cl_2N_2O_2Ru$	$C_{17}H_{22}N_2O_6W$	$C_{23}H_{34}N_2O_6W$
M_r	614.58	534.33	618.38
Crystal appearance	Orange fragment	Yellow plate	Yellow plate
Crystal size/mm	*ca.* 0.15 (irregular)	0.48 × 0.27 × 0.19	0.12 × 0.20 × 0.15
Crystal system	Monoclinic	Monoclinic	Orthorhombic
Space group	$P2_1$	$P2_1$	$P2_12_12_1$
a/Å	7.412(8)	8.165(2)	16.507(4)
b/Å	13.032(4)	24.254(5)	18.696(4)
c/Å	14.438(6)	10.134(2)	8.571(2)
β/°	101.44(3)	93.20(2)	—
U/Å^3	1367(2)	2003.74(3)	2645.14(4)
Z	2	4	4
D_c/g cm^{-3}	1.488	1.771	1.553
μ(Mo-Kα)/cm^{-1}	7.87	55.39	42.02
F(000)	628	1039.81	1231.81
T/K	298	298	298
Diffractometer	Rigaku AFC6S	Philips PW 1100	Philips PW 1100
2θ range/°	2–25	3–25	3–25
Scan width/°	0.65 + 0.35 tan θ	0.9	0.8
Reflections measured	5236	3838	1214
Unique reflections	4843	3628	1214
Observed reflections [$I > 3\sigma(I)$]	4291	2442	857
Maximum, minimum absorption coefficients	1.23, 0.83	1.16, 0.74	1.20, 0.80
hkl Ranges	0–8, −15 to +15, −16 to +16	−9 to +9, 0–28, 0–12	0–9, 0–22, 0–3
R	0.0333	0.0426	0.0552
R'	0.0402	0.0427	0.0566
$(\Delta/\sigma)_{max}$	0.11	0.01	0.01
$(\Delta\rho)_{max}$/e Å^3	0.80	0.98	0.95

and HC^5), 3.49 (2 H, s, central CH_2), 0.96 (6 H, d, J = 7.0, $CHMe_2$) and 0.74 (6 H, d, J = 7.0 Hz, $CHMe_2$). FAB mass spectrum: m/z 534 (11, M^+), 506 (69, M^+ − CO), 478 (15, M^+ − 2CO) and 341 (100%). α(589.3 nm, 1.26, in $CHCl_3$) = +85.5°.

Tetracarbonyl{2,2′-*isopropylidenebis*[(4S)-4,5-*dihydro*-4-*isopropyl*-5,5-*dimethyloxazole*]}*tungsten*(0) **7**.—The compound was prepared in an identical manner to that of **6** in 7% yield, m.p. 163–164 °C (decomp.) (Found: C, 44.8; H, 5.4; N, 4.5. $C_{23}H_{34}N_2O_6W$ requires C, 44.7; H, 5.5; N, 4.5%); ν_{max}(KBr disc) 2979m, 2935w, 2878w (CH), 2000s, 1881s, 1849s, 1817s, 1804 (CO) and 1635 (CN); (CH_2Cl_2) 2005m, 1873s, 1859(sh), 1808s (CO) and 1642m cm^{-1} (CN). ^{1}H NMR (270 MHz, $CDCl_3$): δ_H 3.78 (2 H, d, J = 3.0, CHN), 2.66 (2 H, double spt, J = 7.5, 3.0, C*H*Me$_2$), 1.58 (6 H, s, central CMe_2), 1.52 (6 H, s, Me_2C^5), 1.38 (6 H, s, Me_2C^5), 1.09 (6 H, d, J = 7.5, $CHMe_2$) and 1.02 (6 H, d, J = 7.5 Hz, $CHMe_2$). FAB mass spectrum: m/z 618 (15, M^+), 590 (100, M^+ − CO), 562 (15, M^+ − 2CO) and 530 (7%, M^+ − 3CO − 2H). α(589.3 nm, 0.4, in $CHCl_3$) = +29.9°.

Catalytic Studies.—The catalyst (either 1 mol % complex **2**–**4**, 1 mol % **1** with 4 mol % L^3, or 1 mol % aibn), if used, was added to a solution of styrene (0.15 cm^3, 1.31 mmol) and pentadecane (50 μl, internal standard) in 1,2-dichloroethane (2 cm^3, containing 50 ppm 4-*tert*-butylcatechol if required) using microlitre syringes. Neat Pr^{i}CHO (0.59 cm^3, 6.50 mmol) was added and the reaction stirred under O_2 (1 atm). Alternatively equivalent amounts of Bu^{t}O$_2$H or $NaIO_4$ in toluene and water respectively were added and the reaction stirred in air. Runs with *cis*- and *trans*-stilbene were conducted similarly. Yields of epoxides were determined by GC analysis. Optical purities were assayed by either GC analysis on a Cyclodex-B column at 80 °C (styrene), or for *trans*-stilbene use of tris-{[(3-heptafluoropropyl)hydroxymethylene]-1,7,7-trimethylbicyclo[2.2.1]heptan-2-enato}-europium(III) on samples isolated by preparative TLC (light petroleum–diethyl ether, 9:1).

For kinetic studies high-purity solutions of styrene (5 cm^3, 0.5 mol dm^{-3} in Pr^{i}CHO) and pentadecane (5 cm^3, 0.2 mol dm^{-3} in Pr^{i}CHO) were prepared, mixed and degassed by two freeze–pump–thaw cycles. Oxygen gas (1 atm) was admitted to the frozen reaction mixture and its temperature brought rapidly to 40 °C. The course of the reaction was monitored by GC analysis.

Crystallographic Studies.—Crystals of the ruthenium complex **2** were obtained by cooling of CH_2Cl_2–Et_2O mixtures to −20 °C, while those of the tungsten complexes **6** and **7** were obtained from tetralin–pentane solutions at 4 °C. All samples were mounted on glass fibres using super glue. Details of the crystal and refinement data are presented in Table 8, however it is worth noting that as all of these complexes possess homochiral ligands they crystallise with acentric polar space groups as expected.

Computations for complex **2** were carried out using the data with $F_o^2 > 3\sigma(F_o^2)$, where $\sigma(F_o^2)$ was estimated from counting statistics.[36] Corrections for Lorentz and polarisation effects and for absorption[37] were applied. The position of the metal atom was determined from a Patterson map. Other atoms were located from difference-Fourier syntheses. The refinement and final full-matrix least-squares refinement based on F was carried out using the TEXRAY program set.[38] The function minimised was $\Sigma w(|F_o| - |F_c|)^2$ where $w = 4F_o^2/\sigma^2(F_o^2)$, $\sigma^2(F_o^2) = [S^2(C + R^2B + 0.03F_o^2)^2]/L_p^2$, S = scan rate, C = total integrated peak count, R = ratio of scan time to background counting time, B = total background count and L_p = Lorentz-polarisation factor. Atomic scattering factors for non-hydrogen atoms were taken from ref. 39 and those for hydrogen from ref. 40 The effects of anomalous disperson were included using values for $\Delta f'$ and $\Delta f''$ from ref. 41 The model converged with R = 0.0333, R' = 0.0402 (goodness of fit = 1.68).

The structures of complexes **6** and **7** were also solved and refined by standard techniques.[42,43] The coordinates for the tungsten atoms were deduced from Patterson synthesis and the remaining non-hydrogen atoms located from subsequent Fourier-difference syntheses. The hydrogen atoms could not be located directly and were therefore included in geometrically idealised positions (C–H 1.080 Å) and were constrained to 'ride'

on the relevant carbon atoms, with all hydrogen atoms assigned fixed thermal factors of 0.08 Å^2, but their parameters were not refined. The tungsten atom and both oxygen atoms of the oxazole ligand were assigned anisotropic thermal parameters in the final cycles of full-matrix refinement which converged at $R = 0.0426$ and $R' = 0.0427$ for **6**, and $R = 0.0552$ and $R' = 0.0566$ for **7**, with weights $w = 1/\sigma^2 F_o$ assigned to individual reflections in both cases.

Additional material available from the Cambridge Crystallographic Data Centre comprises H-atom coordinates, thermal parameters and remaining bond lengths and angles.

Acknowledgements

We are grateful to Zeneca, EPSRC and the LINK Asymmetric Synthesis Programme for financial support and a studentship (to S. R.). We thank the EPSRC mass spectroscopy service for FAB mass spectra and Mr. Hamish Robertson for some initial investigations. Johnson Matthey provided a generous loan of ruthenium chloride.

References

1 T. Yamada, T. Takai, O. Rhode and T. Mukaiyama, *Chem. Lett.*, 1991, 1.
2 T. Takai, E. Hata, T. Yamada and T. Mukaiyama, *Bull. Chem. Soc., Jpn.*, 1991, **64**, 2513.
3 S. Inoki, T. Taki, T. Yamada and T. Mukaiyama, *Chem. Lett.*, 1991, 941.
4 T. Yamada, T. Takai, O. Rhode and T. Mukaiyama, *Bull. Chem. Soc., Jpn.*, 1991, **64**, 2109.
5 T. Yamada, K. Imagawa, T. Nagata and T. Mukaiyama, *Chem. Lett.*, 1992, 2231.
6 T. Mukaiyama, T. Yamada, T. Nagata and K. Imagawa, *Chem. Lett.*, 1993, 327.
7 B. Meunier, *Chem. Rev.*, 1992, **92**, 1411.
8 C. Bolm, *Angew. Chem., Int. Ed. Engl.*, 1991, **30**, 542.
9 J. T. Groves and R. Quinn, *J. Am. Chem. Soc.*, 1985, **107**, 5790.
10 M. Tavarès, R. Ramasseul, J.-C. Marchon, B. Bachet, C. Brassy and J.-P. Mornon, *J. Chem. Soc., Perkin Trans. 2*, 1992, 1321.
11 R. A. Leising and K. J. Takeuchi, *Inorg. Chem.*, 1987, **26**, 4391.
12 A. S. Goldstein, R. H. Beer and R. S. Drago, *J. Am. Chem. Soc.*, 1994, **116**, 2424.
13 M. M. T. Khan, A. P. Rao, S. D. Bhatt and R. R. Merchant, *J. Mol. Catal.*, 1990, **62**, 265.
14 K. Kaneda, S. Haruna, T. Imanaka, M. Hamamoto, Y. Nishiyama and Y. Ishii, *Tetrahedron Lett.*, 1992, **33**, 6827.
15 C. Bolm, G. Schlingloff and K. Weickhardt, *Tetrahedron Lett.*, 1993, **34**, 3405.
16 D. Müller, G. Umbricht, B. Weber and A. Pfaltz, *Helv. Chim. Acta*, 1991, **74**, 232.
17 D. L. Evans, D. K. Minster, U. Jordis, S. M. Hecht, A. L. Mazzu and A. I. Meyers, *J. Org. Chem.*, 1979, **44**, 497.
18 E. J. Corey and K. Ishihara, *Tetrahedron Lett.*, 1992, **33**, 6807.
19 R. W. Saalfrank, O. Struck, K. Nunn, C.-J. Lurz, R. Hartbig, K. Peters, H. G. von Schnering, E. Bill and A. X. Trautwein, *Chem. Ber.*, 1992, **125**, 2331.
20 T. V. Ashworth, D. C. Liles, D. J. Robinson, E. Singleton, N. J. Coville, E. Darling and A. J. Markwell, *S. Afr. J. Chem.*, 1987, **40**, 183.
21 C. K. Johnson, ORETP, Report ORNL-5138, Oak Ridge National Laboratory, Oak Ridge, TN, 1976.
22 C. Potvin, J. M. Manoli, G. Pannetier and N. Platzer, *J. Organomet. Chem.*, 1981, **219**, 115.
23 K.-Y. Wong, C.-M. Che, C.-K. Li, W.-H. Chiu, Z.-Y. Zhou and T. C. W. Mak, *J. Chem. Soc., Chem. Commun.*, 1992, 754.
24 R. O. Gould, C. L. Jones, D. R. Robertson and T. A. Stephenson, *J. Chem. Soc., Dalton Trans.*, 1977, 129.
25 C. Potvin, J. M. Manoli, G. Pannetier and R. Chevalier, *J. Organomet. Chem.*, 1978, **146**, 57.
26 W. S. Sheldrick and R. Exner, *Inorg. Chim. Acta*, 1989, **166**, 213.
27 H. R. Cooper and H. W. Melville, *J. Chem. Soc.*, 1951, 1994.
28 G. E. Zaikov, J. A. Howard and K. U. Ingold, *Can. J. Chem.*, 1969, **47**, 3017.
29 R. A. Sheldon and J. K. Kochi, *Metal-Catalyzed Oxidations of Organic Compounds*, Academic Press, New York, 1981.
30 R. R. Diaz, K. Selby and D. J. Waddington, *J. Chem. Soc., Perkin Trans. 2*, 1977, 360.
31 J. C. Dobson, W. K. Seok and T. J. Meyer, *Inorg. Chem.*, 1986, **25**, 1514.
32 R.-Y. Yang and L.-X. Dai, *J. Mol. Catal.*, 1994, **87**, L1.
33 M. Brenner and W. Huber, *Helv. Chim. Acta*, 1953, **36**, 1109.
34 C. C. Price and E. L. Eliel, *J. Org. Chem.*, 1957, **22**, 342.
35 M. O. Albers, T. V. Ashworth, H. E. Oosthizen and E. Singleton, *Inorg. Synth.*, 1989, **26**, 68.
36 P. W. P. Cornfield, R. J. Doedens and J. A. Ibers, *Inorg. Chem.*, 1967, **6**, 197.
37 N. Walker and D. Stuart, *Acta Crystallogr., Sect. A*, 1983, **39**, 158.
38 TEXRAY, Structure Analysis Package, Molecular Structure Corporation, Houston TX, 1985.
39 D. T. Cromer and J. T. Waber, *Acta Crystallogr.*, 1965, **18**, 104.
40 R. F. Stewart and E. R. Davidson, *J. Chem. Phys.*, 1965, **42**, 3175.
41 D. T. Cromer, *Acta Crystallogr.*, 1965, **18**, 17.
42 M. K. Cooper, H. J. Goodwin, P. J. Guerney and M. McPartlin, *J. Chem. Soc., Dalton Trans.*, 1982, 757.
43 G. M. Sheldrick, SHELX 76 program for crystal structure determination, University of Cambridge, 1976.

Received 22*nd July* 1994; *Paper* 4/04493B